ACS APPLIED MATERIALS & INTERFACES

Research Article

www.acsami.org

Ligand Induced Spectral Changes in CdSe Quantum Dots

Jon M. Azpiroz*,†,‡ and Filippo De Angelis*,†

†Computational Laboratory for Hybrid/Organic Photovoltaics (CLHYO), Istituto CNR di Scienze e Tecnologie Molecolari (ISTM-CNR), Via Elce di Sotto 8, 06123, Perugia, Italy

‡Kimika Fakultatea, Euskal Herriko Unibertsitatea (UPV/EHU), and Donostia International Physics Center (DIPC), P. K. 1072, 20080 Donostia, Euskadi, Spain

Supporting Information

ABSTRACT: The rational design of ligand molecules has earned lots of attention as an elegant means to tailor the electronic and optical properties of semiconductor quantum dots (QDs). Aromatic dithiocarbamate molecules, in particular, are known to greatly influence the optoelectronic properties of CdSe QDs, red-shifting the absorption features and enhancing the photoluminescence. Here, we present an integrated computational study, which combines *ab initio* molecular dynamics and excited state calculations including thousands of excitations, aimed at understanding the impact of this kind of surface ligand on the optoelectronic properties of CdSe QDs. We demonstrate that the valence electronic states of the dithiocarbamate molecules, mostly localized in the anchoring moiety, are responsible for the red-shift of the absorption features of capped CdSe QDs. Ligands develop interfacial electronic states close to the band edges of the CdSe, which enhance the absorption features of the QD and might open new channels for the radiative decay from the excited state, improving optical emission. Hybridized QD/ligand states could also funnel interfacial charge transfer between the inorganic core and surface molecules, a process that lies at the heart of many photovoltaic and photocatalytic devices. This work may pave the way toward the design of new capping ligands that, adsorbed on the QD surface, could provide control over the optoelectronic properties of the semiconductor core.

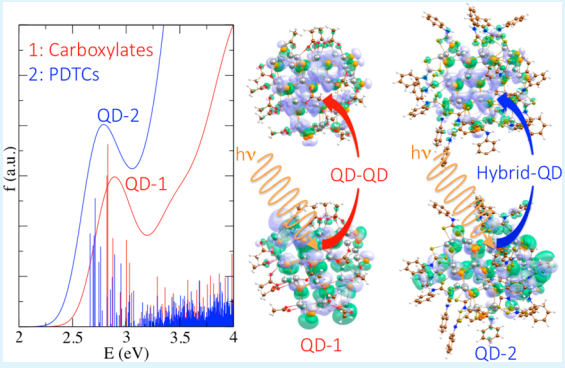

KEYWORDS: *electronic structure, absorption spectra, carboxylate, phenyl dithiocarbamate, DFT, CPMD*

1. INTRODUCTION

Semiconductor quantum dots (QDs) have now been the focus of intense study for about two decades due to their outstanding optical and electronic properties, which might be modified at will through variations of their shape and size.[1−10] QDs are usually synthesized in solution, in the presence of coordinating ligands that dynamically adhere to the surface and control the QD nucleation and growth processes. Furthermore, ligand molecules play a crucial role in capping the unsaturated atoms on the QD surface, which otherwise would give rise to localized orbitals that could trap charge carriers and deteriorate the nanostructure's electronic and optical properties.[5−7,11]

The role of surface molecules is not, however, limited to surface saturation. The binding of certain ligands may strongly influence the QD electronic structure, thus providing an elegant means to finely tune the QD properties.[8,12−15] For instance, amine-capped QDs generally exhibit blue-shifted optical features and enhanced emission properties as compared to their thiol-passivated counterparts, which were proposed to introduce trap states into the intrinsic band gap of the QDs.[8] Moreover, the appropriate alignment of electronic levels might promote interfacial electron/hole transfer between QDs and surface attached molecules,[16,17] a process which holds enormous potential in many fields. As a matter of fact, scavenging the photogenerated carriers from the QD core is the first step of many photocatalytic reactions, including water splitting,[18] alcohol dehydrogenation and hydrogenolysis,[19] and CO_2 reduction.[20] Hole extraction is of crucial importance in photovoltaics because it prevents exciton recombination, a process that competes with the interfacial electron transfer lying at the heart of many solar cell devices.[21,22] Hole scavenging also prevents oxidation and therefore stabilizes the QD.[23] Interfacial electron transfer in QD-based devices could further be enhanced by appropriate ligands that improve the coupling between the donor and the acceptor, e.g., a metal-oxide semiconductor in QD-sensitized solar cells.[24] For instance, aromatic ligands, with their π-conjugated structure, are known to funnel electron injection from QD sensitizers to the metal-oxide substrate.[25]

Phenyl dithiocarbamate (PDTC, Scheme 1a) ligands have earned lots of attention quite recently,[26,27] because they may greatly influence the electronic and optical features of

Received: June 18, 2015
Accepted: August 20, 2015
Published: August 20, 2015

DOI: 10.1021/acsami.5b05418
ACS Appl. Mater. Interfaces 2015, 7, 19736−19745

Scheme 1. (a) Chemical Structure of the Phenyl Dithiocarbamate (PDTC) Ligand; (b) Adiabatic (Solid Arrow, Left) and Nonadiabatic (Dashed Arrow, Right) Mechanisms for Hole Transfer from QDs to Surface Attached PDTC Ligands

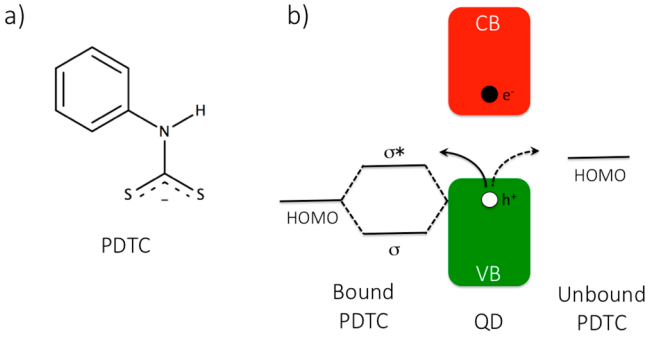

semiconductor QDs.[28−31] The absorption spectra of PDTC-capped CdSe QDs display a sizable red-shift with respect to their native counterparts, covered with carboxylate-terminated insulating ligands, e.g., oleic acid.[28,30] Such an increase of the apparent QD radius has been attributed to the delocalization of the exciton over the ligand shell. Weiss and co-workers[28,30] have suggested that the HOMO levels of the PDTC ligands coincide with the valence band (VB) edge of the CdSe QDs. Such a resonance condition may lead to interfacial QD-ligand states (both bonding and antibonding combinations, Scheme 1b), which in turn could funnel hole delocalization from the inorganic core to the ligand shell. The orbitals of carboxylate-terminated insulating ligands lie far from the band edges of the QDs, and no such relaxation of the exciton is thus predicted. This difference led to a sizable absorption red-shift (0.13 eV) in PDTC- vs carboxylate-functionalized CdSe QDs.[28]

p-substituted PDTC ligands have also been studied,[29,31] and it has been found that the chemical nature of the *p*-substituent plays a key role in the optoelectronic properties of the QD. In all cases, a red-shift of the QD absorption edge is found compared to carboxylate-functionalized QDs, but the magnitude of the red-shift increases when passing from electron-donating groups (EDG), e.g., OCH_3, to electron-withdrawing groups (EWG), e.g., CF_3. The major effect of changing the *p*-substituent from EDG to EWG is to stabilize the ligand HOMO in such a way that it becomes aligned with a denser manifold of occupied states of the QD, and a more destabilized (antibonding) interfacial state is created.[29]

Delocalizing the exciton into the ligand shell is also reflected in the emission characteristics of the QD. As recently shown by Tan et al.,[32] hole transfer from CdSe QDs to surface attached PDTC ligands quenches the photoluminesce (PL) of the inorganic core. According to these experiments, ligands bearing EDGs are better hole scavengers, due to their higher-lying HOMO. This finding is in apparent contradiction with previous results showing that PDTCs with EWGs delocalize the positive charges more efficiently. Weiss and co-workers have reconciled this apparent discrepancy in a very recent work, in which the role played by the bound/unbound ligands has been disentangled.[33] From their results, unbound PDTCs molecules present in the QD solution (and related degradation products) are responsible for the PL quenching. Therefore, ligands bearing EDGs, with their higher-lying HOMO, should better scavenge holes from the QD, due to an increasing driving force. Such a nonadiabatic charge transfer is in sharp contrast with the

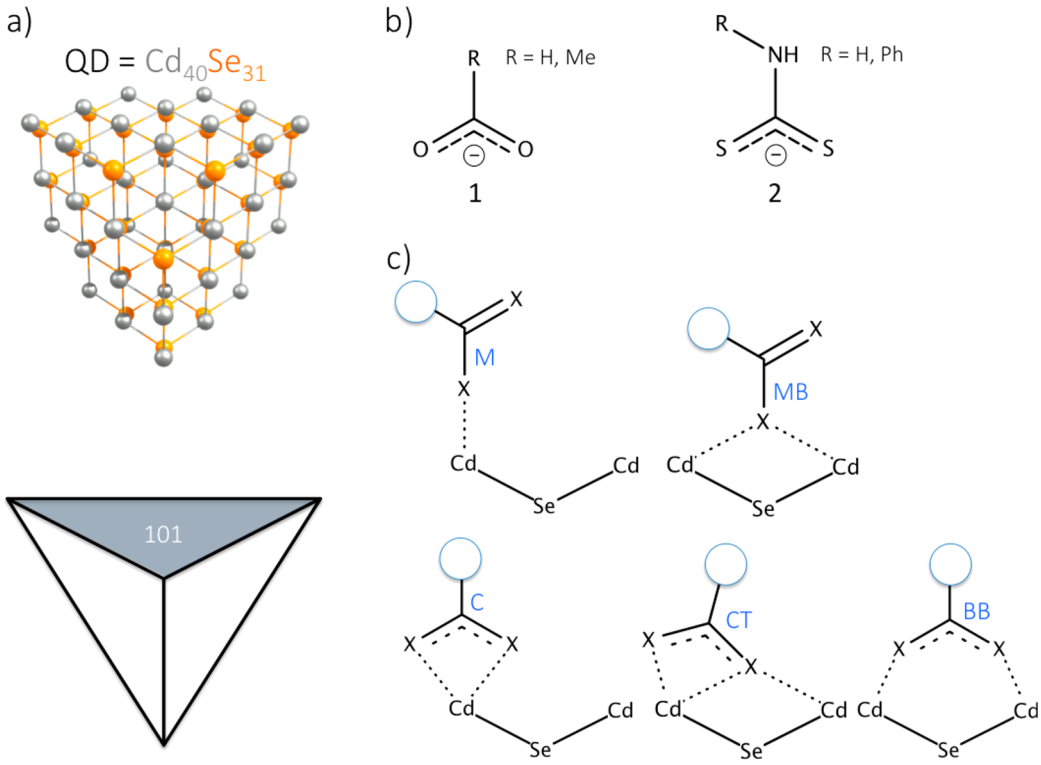

Figure 1. (a) Geometry of the $Cd_{40}Se_{31}$ cluster, exposing a majority Cd-rich (101) surface, as sliced from the underlying zinc-blende crystal structure. Gray = Cd and orange = Se atoms. (b) Ligand models used in this study to represent the long chain acids (**1**) and dithiocarbamate (**2**) molecules used experimentally. (c) Possible anchoring geometries of **1** and **2** on the CdSe surface.

DOI: 10.1021/acsami.5b05418
ACS Appl. Mater. Interfaces 2015, 7, 19736−19745

interfacial state-mediated (adiabatic) hole delocalization induced by the bound ligands; see Scheme 1b.

As a matter of fact, surface attached PDTC molecules have been shown to enhance the QD PL, by increasing the rate of radiative exciton decay. Accordingly, the intensity of the lowest-energy peak in the absorption spectrum increases in passing from carboxylate- to PDTC-capped QDs.[33] However, it is still unclear whether an increase in the density of excited states (i.e., the number of excited states per energy unit) or an increase in the intensity of formerly dark transitions is responsible for such an enhancement.

Here, we present an integrated computational study of realistically large ligand-capped CdSe QDs, which combines *ab initio* molecular dynamics and excited state calculations, aimed at understanding the impact of surface molecules on the optoelectronic properties of the inorganic core. In particular, we demonstrate that the HOMO levels of the PDTC molecules, mostly localized in the anchoring dithiocarbamate moiety, are responsible for the red-shift of absorption features of PDTC-capped CdSe QDs compared to their carboxylate-functionalized analogues, in agreement with the mechanism suggested by Weiss and co-workers.[29] PDTC molecules develop interfacial electronic states close to the band edges of the CdSe, which enhance the QDs optical features and may open new relaxation channels for the photoexcited charge carriers. Moreover, hybridized QD/ligand states could also funnel hole/electron transfer between the inorganic core and surface molecules, a process that lies at the heart of many photovoltaic and photocatalytic devices. We furthermore demonstrate the importance of the ligands' adsorption mode and their dynamics on the QD surface in determining the QDs' optical absorption features.

2. MODEL AND METHOD

To simulate the CdSe QDs, a 1.5 nm size $Cd_{40}Se_{31}$ cluster exposing a majority Cd-rich (101) surface has been sliced from the underlying zinc-blende crystal structure; see Figure 1a. With a Cd/Se ratio of ca. 1.3 and pyramidal shape, our model reproduces the stoichiometry and the morphology of the experimental QDs.[34] To ensure charge neutrality of the model, 18 anion ligands (i.e., carboxylate, **1**, or dithiocarbamate, **2**) have been placed on the QD surface; see Figure 1b. To explore the conformational space of the passivated QDs and sample the diverse binding modes of the ligands on the nanostructure surface, Car-Parrinello molecular dynamics[35] (CPMD) simulations have been carried out, employing the PBE functional[36] in conjunction with a plane wave basis set (25/240 Ry cutoff for wave functions and augmented charge density) and ultrasoft pseudopotentials,[37,38] as implemented in the Quantum Espresso package.[39] Electron−ion interactions were described by scalar relativistic ultrasoft pseudopotentials with electrons from Cd 4d5s; Se 4s4p; H 1s; C, N, O 2s2p; and S 3s3p shells explicitly included in the calculations. CPMD simulations have been performed with an integration time step of 10 au. The fictitious mass used for the electronic degrees of freedom is 1000 au, and we set the atomic masses to an identical value of 5 amu, to enhance the dynamical sampling. Initial randomization of the atomic positions has been used to reach a temperature of 300 ± 20 K, without further applying any thermostat. Dynamics simulations have been performed in cubic supercells of side 23 and 25 Å for the **1**- and **2**-capped QDs, respectively. For computational convenience, CPMD simulations were conducted by replacing the ligand R groups by H atoms; see Figure 1b.

Suitable structures extracted from the CPMD dynamics have been further optimized by PBE in conjunction with the SBKJC-VDZ basis set,[40] as implemented in the TURBOMOLE6.3 package.[41] To better represent the surface molecules employed experimentally (i.e., OA and PDTC), ligand R groups are now modeled by Me and Ph groups, respectively; see Figure 1b. Although possibly reliable for geometries and energetics, GGA functionals such as PBE suffer from well-known problems in describing semiconductor band gaps and interfacial alignment of energy levels.[42] Therefore, we utilize the hybrid PBE0 functional,[43] in conjunction with the same SBKJC-VDZ set, to perform single point calculations on top of the PBE-optimized geometries and subsequent excited state calculations. The effect of solvation has been included implicitly by means of the COSMO model.[44] To reproduce the experimental measurements,[31,33] the dielectric constant has been set to 8.93, which corresponds to CH_2Cl_2. To simulate the optical absorption of the ligand-capped QDs, we take advantage of the simplified Tamm Dancoff Approach (sTDA) recently developed by Grimme et al.,[45] which allows the calculation of thousands of excitations in extended systems. In such a way, we are able to simulate the optical features of the title systems up to 5 eV, providing a direct comparison with the experiment. Preliminary calculations revealed that the sTDA approach is able to nicely reproduce the TDDFT absorption onset of ligand-capped CdSe QDs, with maximum deviations within 0.02 eV; see Figure S1. All the hybrid calculations have been carried out in the TURBOMOLE6.3 package.

3. RESULTS AND DISCUSSION

3.1. Structure and Energetics. In Figure 2, the first production snapshots taken from the CPMD simulations are shown, after geometry optimization. As it is immediately clear, the QDs undergo a modest reconstruction with respect to the pristine zinc-blende cluster, preserving the bulk-like crystal structure. This is in sharp contrast with bare QDs, which experience drastic atomic rearrangements on the surface, affecting even the inner part of the nanostructure. Surface ligands saturate the dangling atoms on the CdSe surface, lowering the surface energy and stabilizing the whole QD. As one might notice from Figure 2, the geometry of the CdSe core is quite similar for the **1**- and **2**-capped models, meaning that the surface speciation plays a minor role in the atomic structure of the QD.

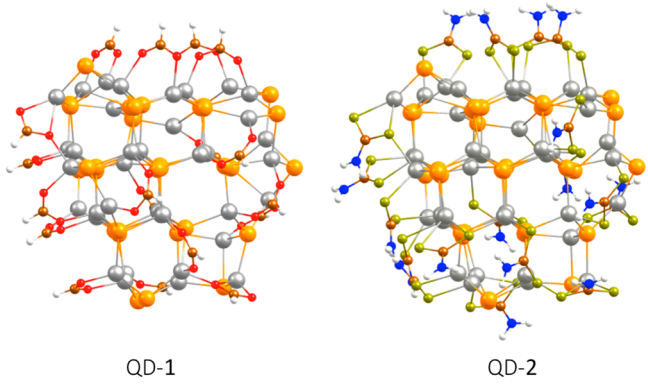

Figure 2. Optimized geometries of the QD-**1** and QD-**2** compounds, relaxed from the first production snapshot of the molecular dynamics simulations. Note that R groups in ligands are modeled with H atoms. Gray = Cd, orange = Se, red = O, brown = C, white = H, yellow = S, and blue = N atoms.

The ligands may adopt different interacting geometries and binding modes on the QD surface. In Figure 1c, we draw the anchoring modes sampled during the CPMD simulations, namely, monodentate (M), monodentate bridged (MB), chelating (C), chelating tilted (CT), and bidentate bridged (BB). As one might notice from Figure 2, BB seems to be the prevalent adsorption mode for both **1** and **2**, with 16 and 12 molecules anchored in such a way in QD-**1** and QD-**2**,

DOI: 10.1021/acsami.5b05418
ACS Appl. Mater. Interfaces 2015, 7, 19736−19745

respectively. Two **1** molecules adopt the CT structure, as four **2** ligands do. Finally, there is a single **2** molecule exhibiting the C anchoring mode. In previous theoretical works, the energy difference between the distinct interacting modes has been calculated to be small.[46,47] Accordingly, ligands are supposed to assume different anchoring geometries over the CPMD trajectory.

Our molecular dynamics simulations confirm such a hypothesis for the QD-**2** system; see Figure 3b. The surface

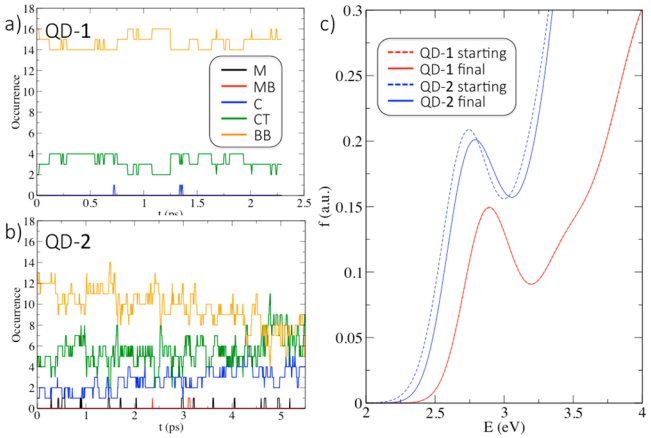

Figure 3. Number of ligands adopting monodentate (M), monodentate bridge (MB), chelating (C), chelating tilted (CT), and bidentate bridge (BB) anchoring geometries along the Car-Parrinello molecular dynamics simulations for QD-**1** and QD-**2**, (a) and (b), respectively. (c) Simulated absorption spectra of the starting optimized (first, dashed lines) and the final optimized (last, solid lines) geometries taken from the molecular dynamics for QD-**1** (red lines) and QD-**2** (blue lines). Note the solid and dashed lines in QD-**1** are essentially superimposed.

2 ligands behave fluxionally, switching between the distinct binding modes. During the dynamics, which cover ca. 5 ps, the number of molecules assuming the C and CT geometries increases at the expense of those at the BB configuration. Running the simulation of the QD-**2** complex longer might result in further changes. However, this run suffices to demonstrate the mobile nature of dithiocarbamate ligands. As it is clear from Figure 3b, QD-**1** behaves as a more rigid system, and the **1** ligands stay predominantly at the BB conformation. Note that for the **1**-capped model a shorter production run of ca. 2.5 ps has been carried out, enough to corroborate that **1** molecules behave quite rigidly. Single point calculations at the optimized geometries reveal that **1** molecules adsorb more strongly on the QD surface (with a calculated binding energy of 79 kcal/mol) than the **2** (74 kcal/mol), which is consistent with the more static behavior of the carboxylate ligands.

Different CPMD simulations would be necessary to better sample the conformational space of the ligand-capped QDs. This poses a serious computational challenge, which could better be tackled by classical molecular mechanics (MM) simulations. On the basis of a simple electrostatic model to represent the ligand−nanocrystal interaction, some authors were able to reproduce the binding energies calculated by means of quantum chemical approaches and to disentangle the dynamics of the ligand (amine) adsorption on the CdSe surface.[48] However, this kind of electrostatic model is not able to properly describe the covalent nature of the ligand−nanocrystal bond and hardly accounts for the bond formation/breaking events that take place between the surface ligands and the inorganic QDs. Reactive force fields seem to be better suited for this purpose. This kind of approach could be very useful to explore the conformational space of the ligand-capped CdSe QDs, in search of the lowest-lying structure.

Anyway, for both QD-**1** and QD-**2**, suitable structures taken during the dynamics give rise to almost isoenergetic conformers upon geometry optimization (irrespective of R), even in the cases in which surface ligands adopt distinct interacting geometries, suggesting a quite flat energy landscape for this kind of ligand-protected QD. Notably, however, the last snapshot of the CPMD simulation gave rise to the most stable conformer in both **1**- and **2**-capped QDs. The inorganic core remains relatively unchanged during the dynamics, in contrast to previous works,[13,49] in which bare QDs experience sizable structural changes during the simulation. This is due to surface ligands which saturate undercoordinated QD atoms on the exposed facets.

From these results, the energy of the ligand-capped QDs seems to be quite insensitive to the anchoring mode of the surface molecules. However, the latter could still play a role on the electronic and optical properties of the nanocomposite. As a matter of fact, the optoelectronic properties of dye-sensitized semiconductors are largely affected by the anchoring mode of the sensitizer.[51] Therefore, in a first approach, we monitored the energy of the HOMO level of QD-**1** and QD-**2** along the CPMD simulation; see Figure S2. We assume here that the PBE functional should fairly reproduce the effect of the structural dynamics on the electronic properties of the title compounds. The mobility of the dithiocarbamate ligands is clearly reflected in the HOMO level of QD-**2**, which sizably

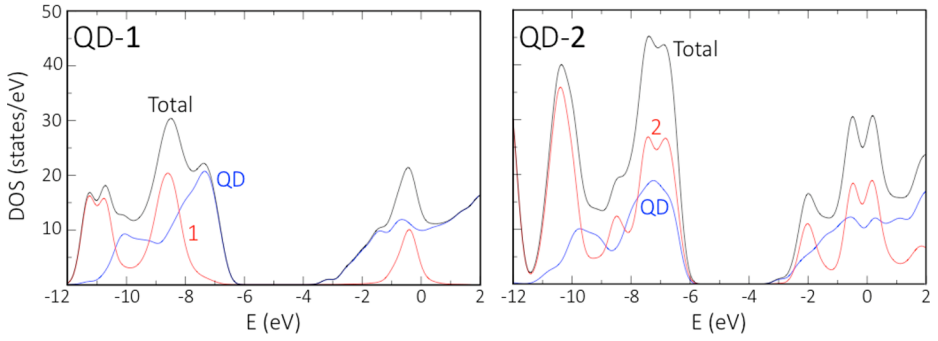

Figure 4. Density of states (DOS, black) of the QD-**1** (left) and QD-**2** (right) complexes, obtained by a Gaussian convolution of σ = 0.2 eV of the individual molecular orbitals. The projection of the DOS (PDOS) on the CdSe core (solid blue) and the ligand shell (solid red) is also shown.

DOI: 10.1021/acsami.5b05418
ACS Appl. Mater. Interfaces 2015, 7, 19736−19745

oscillates during the CPMD simulation. The HOMO oscillates to a lesser extent for the QD-**1** model, due to the more rigid behavior of the carboxylate molecules.

In Figure 3c, we report the optical spectra of the first and the last geometries taken from the CPMD dynamics, once capped with the ligands bearing the R = Me, Ph groups and optimized. As it is immediately clear, the absorption features of QD-**1** are almost identical for the two considered structures, due to the very similar adsorption pattern of the surface ligands. QD-**2** delivers a different picture, consistent with the fluxional behavior of the dithiocarbamate ligands on the CdSe surface. In particular, the first excitonic feature experiences a blue-shift of ca. 0.05 eV during the dynamics. Since the ligand-induced spectral changes in CdSe QD amount to just 0.1−0.2 eV, in order to provide a direct comparison with the experiments, the choice of the appropriate isomer seems to be crucial.

The experimental spectra will probably correspond to an average of the conformations sampled by the capped QD during the simulation time. Therefore, the best comparison with the experiment might necessitate an exhaustive sampling of the configurational space of the nanostructure. With the calculations presented here, however, we are able to demonstrate that the thermal motion plays an important role on the absorption spectra of the title compounds and that the most stable isomers better reproduce the experimental results. Similarly, Lee et al. found that the XAS spectra of ligand-capped CdSe QDs strongly depend on the interacting geometry of the surface molecule.[52]

3.2. Electronic Structure. To understand the electronic structure of the **1**- and **2**-capped QDs, in Figure 4, we depict their density of states (DOS). For comparison, we also calculated the DOS of the bare QDs, calculated at the geometry they assume in the interacting complexes; see Figure S3. Since the bare QD bears a net charge of +18 lel, its VB and CB are shifted to lower energies by ca. 7 eV with respect to the ligand-capped (neutral) QD. In order to compare both cases, we perform a rigid shift of the DOS of the bare QD, in such a way that the d orbitals of Cd, which are supposed to be quite insensitive to surface speciation,[53] match with the d shell of the passivated QDs.

Bare QDs exhibit a quite similar DOS, with calculated HOMO−LUMO gaps of 2.35 and 2.39 eV at the QD-**1** and QD-**2** geometries, meaning that the electronic structure is quite insensitive to the particular structure adopted by the CdSe core due to the surface molecules. Interestingly, no trap states are observed at the edges of the VB and the CB. It seems that, even in the presence of the coordinating ligands, there is a surface reconstruction, which prevents the development of localized states. Ligand adsorption produces a sizable opening of the band gap, due to the destabilization of the CB edge and the stabilization of the VB edge, which leave the HOMO−LUMO differences of 3.54 and 3.32 eV for QD-**1**.Me and QD-**2**.Ph, respectively. The CB edges experience a shift of ca. 0.3 eV, which leave the LUMO at −3.17 and −2.96 eV, respectively. The VB edge levels of QD-**1**, instead, are 0.45 eV deeper than those of QD-**2**, which results in a blue-shifted band gap.

Irrespective of the surface molecules, the shape of the DOS at the band gap edges changes notably upon ligand adsorption. To gain insight on the electronic structure of the passivated QDs, we have calculated the projection of their DOS (PDOS) on the inorganic core and the surface ligands; see Figure 4. In Figure 5, instead, we have sketched the band gap edge electronic levels of the interacting complexes, along with the

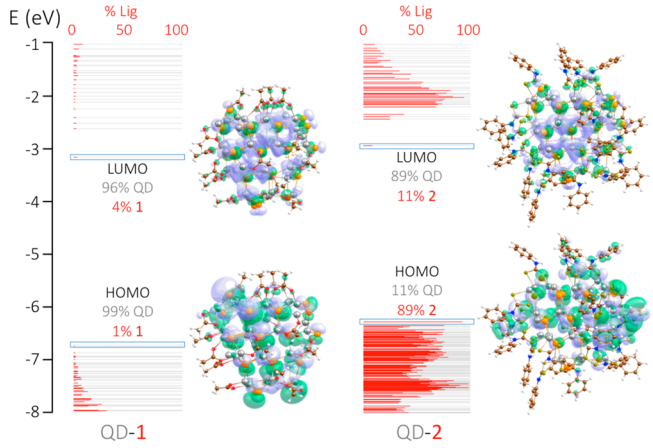

Figure 5. Electronic levels (gray sticks) of the QD-**1** (left) and QD-**2** (right) complexes, along with their projection on the surface ligands (red sticks). The HOMO and LUMO levels are highlighted, and the corresponding isodensity plots depicted.

contribution of the ligand shell to each of the molecular orbitals. As it is immediately clear from this representation, the title compounds display three types of states: (i) the ones mostly localized in the QD core (with a ligand contribution smaller than 25%); (ii) those spread over the ligand shell (with a ligand contribution greater than 75%); (iii) interfacial QD/ligand states (with a ligand contribution between 25% and 75%), which involve a strong hybridization of the QD and the ligand orbitals.

From Figures 4 and 5, the VB and the CB edges of QD-**1** are localized in the CdSe core. The ligands contribute deep inside the bands, as suggested by previous experiments.[29] Deeper in the bands, ligand and CdSe orbitals couple electronically, leading to mixed states that spread over the whole nanocomposite. Only deep in the VB and the CB, where no CdSe states contribute, pure ligand states appear; see Figure 4. Our results are in good agreement with those reported by Voznyy in his work about CdSe nanocrystals passivated with carboxylic acids.[46] He demonstrated that, for charged-balanced QDs, the ligand states appear deep inside the VB and the CB. He also showed that excess ligands can produce surface trap states even in QDs with no dangling bonds on the surface.

QD-**2** delivers a quite different picture, because the orbitals of the aromatic molecules on the QD surface lie close to the band edges of the CdSe. In particular, it seems that the ligand VB edge intrudes into the band gap of the inorganic core, which could explain the red-shift of the absorption features observed experimentally upon the adsorption of **2** molecules. Accordingly, the HOMO of the interacting complex is spread over the ligand shell; see Figure 5. Regarding the CB, the LUMO of QD-**2** is mostly localized in the CdSe core. Higher-lying CB states, however, show an important contribution from the surface ligands. The efficient electronic coupling between the ligand and the CdSe states gives rise to interfacial QD/ligand orbitals in the VB edge. Nevertheless, unlike QD-**1**, the maxima of CdSe and ligand PDOS coincide; see Figure 4, giving rise to a large number of hybridized orbitals.

To unveil the nature of these new interfacial states, we have calculated the overlap population density of states (OPDOS); see Figure S4, which indicates the bonding/antibonding character of a given state. Positive and negative values in the OPDOS correspond to bonding and antibonding interactions

DOI: 10.1021/acsami.5b05418
ACS Appl. Mater. Interfaces 2015, 7, 19736−19745

between the fragment orbitals, respectively. From our calculations, the VB edge states of QD-**2** split into two subsets: (i) the lowest-lying ones, which are bonding in nature; (ii) the highest-lying ones, which are antibonding. This picture is in line with the predictions made by Weiss and co-workers[29] and with Scheme 1.

To guide the rational design of ligands with desired properties, it is interesting to establish a relation between the chemical and the electronic structures of the surface molecules. Therefore, we have calculated the contribution of the different functional groups to the ligand PDOS. In particular, we have projected the electronic levels into the anchoring and the pending moieties of **1** and **2**; see Figure S5. Alongside, we have also computed the contribution of the Cd and the Se atoms to the QD PDOS. For **1**, the anchoring $-COO^-$ group contributes ca. 1.4 eV below the VB edge. The states related to the pending Me moiety are located much deeper in the VB (3.9 eV below the edge). Regarding the CB, the ligand contribution corresponds to $-COO^-$ exclusively, with no participation from Me. For **2**, the ligand states at the VB edge are mainly related to the anchoring $-NHCSS^-$ group, which are hybridized with the Se states of the inorganic core. However, there is also an important contribution from the attached Ph moiety. In fact, the N lone pair allows the resonance of the −CSS and the Ph orbitals.

3.3. Optical Properties. Figure 6 depicts the simulated optical spectra of the QD-**1** and QD-**2**. For completeness, the density of transitions (DOT) is also drawn, which is indicative of the number of electronic excitations occurring in a given energy range. To draw the DOT, the same intensity has been assigned to each of the transitions. In this case, we use the averaged oscillator strength in such a way that the optical spectrum and the DOT integrate to the same number.

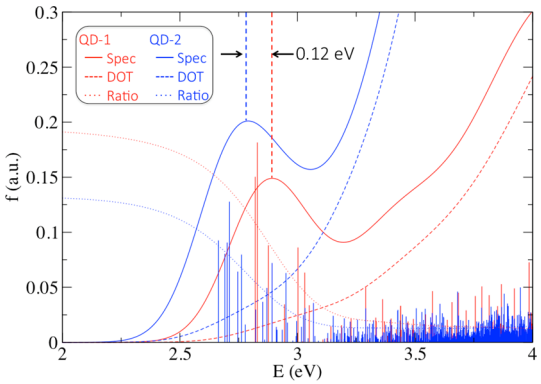

Figure 6. Simulated absorption spectra (Spec, solid lines) of QD-**1** (red) and QD-**2** (blue) complexes, obtained by a Gaussian convolution of σ = 0.15 eV of the individual electronic excitations, which are shown as vertical sticks. For comparison, the density of transitions (DOT, dashed lines) and the Spec/DOT ratio (Ratio, dotted lines) are also shown.

As is immediately clear from Figure 6, the first absorption feature of QD-**2** is red-shifted by 0.12 eV (2.68 vs 2.90 eV) as compared to QD-**1**, in good agreement with the experimental shift of 0.13 eV (2.30 vs 2.43 eV) reported by Weiss and co-workers.[28] Note that the absolute values of the absorption features are blueshifted by ca. 0.4 eV with respect to the experiment due to the reduced size of our model, in which quantum confinement effects are more pronounced.

The second eye-catching feature is the enhancement of the lowest absorption band induced by the aromatic ligands, in line with measurement by Weiss and co-workers, who reported an increase of 1.4 of the integrated extinction coefficient of the first optical feature in PDTC-capped CdSe QDs.[33] More recently, Giansante et al. found a similar ligand-induced spectral change in PbS QDs.[54] By fitting the lowest-energy peak with a single Gaussian, as in ref 33, we find a ratio of ca. 1.5; see Figure S6, in excellent agreement with the experimental value. As suggested in ref 33, two factors might contribute to the enhancement of the lowest absorption feature: (i) an increment in the number of states involved in the electronic transitions and (ii) an increase in the intensity of formerly dark excitations.

As one might notice from Figure 6, the intensity of the electronic transitions is roughly the same for QD-**1** and QD-**2**. Actually, the lowest-lying excitations of QD-**1** are brighter, as shown by the ratio between the spectra and the DOT, which should be indicative of the intensity of the transitions in a given energy range. However, QD-**2** displays a much higher DOT at the first excitonic feature, meaning that many more transitions are involved. As shown in the previous section, ligand **2** molecules introduce occupied states close to the VB edge of the CdSe QD, which contribute decisively to the optical spectrum. These new interfacial states, which enhance the lowest-lying absorption features, could open new radiative relaxation channels for the photoexcited charge carriers and should therefore improve the photoluminescence, as found experimentally.[33]

To gain insight into the main optical features of the title compounds, we partitioned their absorption spectra depending on the CB state accepting the photoexcited electron. From Figure 7a,b, the first excitonic feature (also known as the $1S_e$ state, according to the effective mass approximation)[55] corresponds to transitions from high-lying occupied orbitals

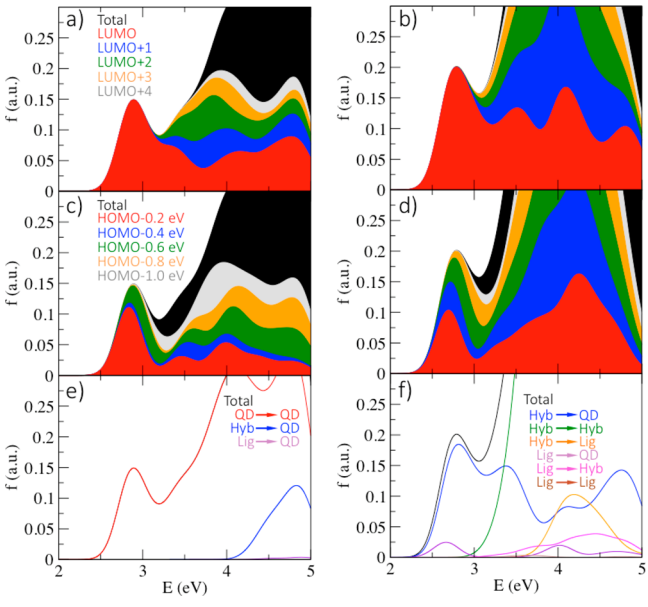

Figure 7. Partition of the absorption spectrum of QD-**1** (left panels) and QD-**2** (right panels): a function of the final CB state (top), the energy of the initial VB state (middle), and the nature of the states involved in the electronic transition (bottom). For the first two partitions (a–d), the weight of each term is proportional to the corresponding colored area. For the third partition (e, f), instead, it is proportional to the height of the curve.

DOI: 10.1021/acsami.5b05418
ACS Appl. Mater. Interfaces 2015, 7, 19736–19745

to the LUMO exclusively, irrespective of the surface ligand. In fact, as is evident from Figure 5, the LUMO lies well separated from the rest of the CB orbitals, even if all share a similar nature. Higher-lying virtual states start contributing ca. 0.5 eV above the absorption onset. According to our calculations, the lowest-lying excitations create hot holes, rather than hot electrons. These highly excited holes, when transferred to the appropriate catalyst, may promote reduction reactions on the surface of the QD. Alternatively, Auger-like energy transfer from photoexcited holes to electrons residing in the LUMO might promote these latter to higher lying conduction states,[56] providing an additional driving force for reduction reactions or interfacial electron transfer processes in photovoltaic devices.

For completeness, we also partitioned the absorption spectra depending on the energy of the VB state from which the electronic excitation takes place. From Figure 7c, the occupied states mainly contributing to the first absorption peak of QD-**1** are located quite close to the VB edge. As a matter of fact, the valence orbitals located in an energy range of 0.2 eV below the HOMO almost shape the lowest excitonic feature of the spectrum. For the QD-**2** model, instead, lower-lying occupied orbitals decisively contribute to the first optical peak.

A third partition which could help in understanding the fine structure of the absorption features depends on the nature of the orbitals involved in the electronic transitions. In Figure 5, we distinguished three classes of orbitals, localized either in the inorganic core (QD) or in the ligand shell (Lig) or spread over the whole interacting complex (Hyb). Accordingly, nine types of electronic transitions might be envisioned, i.e., the QD−QD, Lig−Lig, and Hyb−Hyb excitations and the six mixed terms. In Figure 6c,d, the contribution of each of this terms to the overall optical spectra are shown.

As is immediately clear, the absorption features of QD-**1** correspond to QD−QD transitions. In fact, the VB and the CB edges are localized on the inorganic core when **1** is adsorbed on the QD surface. Therefore, for excitation energies lower than 4 eV, the photoexcited carriers remain in the inorganic core and hardly contribute to the functioning of photovoltaic devices of photocatalytic systems. Only deep in the simulated spectrum (ca. 1.5 eV above the absorption onset), ligand states contribute. In particular, Lig−QD excitations are observed, which correspond to the electron injection from the surface molecules to the CdSe core. Interestingly, the unpaired hole in the carboxylate ligands might promote oxidation reactions. However, the optical spectrum component coming from Lig−QD is lower than the corresponding DOT; see Figure S7, meaning that this kind of electronic transition is quite unlikely. To the contrary, the QD−QD spectrum component lies above the DOT, showing that excitations inside the inorganic core are in general bright, due presumably to the spatial overlap between the occupied and the virtual states involved in the transition. This is particularly true for the first excitonic feature, meaning that the brightest transitions involve the LUMO level.

The peculiar electronic structure of QD-**2** is reflected in its absorption spectrum. As one might notice from the Figure 7d, the first excitonic feature is mostly composed of Hyb−QD excitations. This is consistent with Figure 4, in which the VB edge states of QD-**2** arise from the mixing of the QD and the ligand orbitals. The LUMO, instead, is confined in the inorganic core. With increasing excitation energy, the Hyb−Hyb term dominates. With regard to the intensities of the transitions, see Figure S7, the Hyb−QD excitations responsible for the first absorption peak are quite bright, similar to QD-**1**.

To better understand the outcome of our calculations, we divided the QD-**2** electronic states in two main sets: (1) those mainly localized in the QD core and (2) those localized on the surface ligands. We also decompose the optical spectrum into four main contributions, i.e., those arising from QD−QD, Lig−QD, QD−Lig, and Lig−Lig calculations; see Figure S8. According to these new partitions, the lowest-lying excitations of the **2**-capped QD imply electronic transitions from the PDTC ligands to the CdSe core. Therefore, in agreement with the experiments,[33] under illumination photoexcited holes should delocalize on the surface molecules. Interestingly, these excitations are quite bright, due probably to the favorable electronic coupling between the QD and the ligand states. Higher in energy, pure QD−QD and Lig−Lig excitations contribute. Lig−QD terms appear deeper in the spectrum, suggesting that interfacial electron injection from surface attached PDTC molecules to the CdSe QD might also occur at very high excitation energies.

4. SUMMARY AND CONCLUSIONS

In summary, we have reported a comprehensive computational study, which combines *ab initio* molecular dynamics and excited state calculations including thousands of excitations, aimed at understanding the impact of surface molecules on the properties of CdSe QDs. In particular, we have studied the role played by carboxylate (**1**) and dithiocarbamate (**2**) ligands on the optoelectronics of the inorganic material.

From the dynamics, the **2**-capped QD is predicted to behave as a fluxional system, with surface ligands switching between different adsorption geometries. The **1**-passivated model seems to be more rigid, and ligands remain at the prevalent bidentate bridge anchoring mode. Irrespective of the nature of the surface molecules, the inorganic core stays quite unchanged during the dynamics, in sharp contrast with previous studies on bare systems,[11,50] where QDs were predicted to undergo deep structural rearrangement. Therefore, surface ligands stabilize the bulk-like geometry and prevent the formation of dangling bonds on the surface, which could otherwise act as trap states for the photogenerated carriers. The anchoring geometry of the ligand molecules plays an important role on the optical properties of the title compounds. The different isomers taken from the dynamics, in spite of being almost isoenergetic, differ in their first excitonic feature by 0.05 eV. Since the experimental shifts due to the ligands amount to 0.1−0.2 eV, the choice of the appropriate conformation seems to be crucial in order to provide a meaningful comparison.

The adsorption of surface molecules shapes the band edges of the CdSe QD. Irrespective of the nature of the surface ligand, passivation widens the intrinsic band gap of the inorganic core. For the **1**-capped model, the ligand electronic states are located deep inside the VB and the CB of the CdSe QD. The frontier orbitals of the interacting complex are therefore localized in the inorganic moiety. The **2**-passivated cluster delivers a drastically different picture, because the frontier orbitals of the aromatic molecules appear close to the band edges of the QD. In particular, the ligand HOMOs intrude into the band gap of CdSe. Below the HOMO, the orbitals of the interacting complex comprise a notable mixing between CdSe and ligand states and should therefore funnel photogenerated hole transport from the inorganic core to the ligands. Similar hybrid interfacial states are observed in the CB edge of the **2**-capped QD, which could in turn assist the transfer of photoexcited electrons between the CdSe and the attached molecules.

DOI: 10.1021/acsami.5b05418
ACS Appl. Mater. Interfaces 2015, 7, 19736−19745

Delocalizing electrons/holes in surface ligands holds great potential in photovoltaics, because it allows photogenerated charge carriers to scavenge from QDs. For example, ligand-mediated hole extraction could play a crucial role in the development of new QD sensitized solar cells (QDSSCs) avoiding exciton recombination, a mechanism limiting the device performance.[21,22] Aromatic ligands similar to **2**, with their conjugated structure, should also funnel electron injection from QDs into a metal oxide substrate, a key process in QDSSCs.[24,25] Appropriate ligands could also improve charge carrier conduction in QD-assembled solids, assisting charge hopping between neighboring QDs.[57] From a different perspective, electron/hole extraction could promote reduction/oxidation reactions in the surface attached molecules.[17,19,20] Finally, interfacial charge transfer is also beneficial from the stability point of view, because hole extraction from the QD prevents the oxidation of the nanostructure.[23,32]

The surface ligands leave their fingerprint on the optical features of the title compounds. The intrusion of the **2** HOMO levels into the intrinsic band gap of the CdSe core gives rise to a sizable red-shift of the absorption onset relative to the **1**-capped model, which amounts to 0.12 eV, in good agreement with the experimental number (0.13 eV).[28] The adsorption of PDTC ligands also leads to a notable enhancement of the first excitonic peak, as recently reported by Weiss et al.[33] According to our calculations, the new electronic states developed by the **2** ligands close to the band edges of the CdSe are responsible for such an increase in intensity of the lowest-lying absorption features. The intensity of the electronic transitions remains roughly the same when passing from the **1**-capped to the **2**-passivated model. Importantly, the interfacial ligand/QD states developed at the VB edge of QD-2 could open new relaxation channels for the photoexcited charge carriers and therefore assist the radiative recombination of the exciton. The interfacial states dominate the absorption spectrum of the **2**-capped CdSe QD. On the contrary, the states involved in the lowest-lying electronic excitations of **1**-covered QD are localized in the inorganic core.

We believe that this work paves the way for the *in silico* design of new capping ligands that, adsorbed on the QD surface, would funnel charge extraction from the inorganic core. Such a control over the interfacial charge transfer hold enormous potential in a wide variety of fields, including photocatalysis and photovoltaics.

■ ASSOCIATED CONTENT

Supporting Information

The Supporting Information is available free of charge on the ACS Publications website at DOI: 10.1021/acsami.5b05418.

Figure S1, simulated sTDA and TDDFT spectra of the ligand-capped $(Cd_{56}Se_{50})\cdot 12$ **1** QD; Figure S2, evolution of the HOMO energies of the QD-**1** and QD-**2** complexes along the CPMD trajectories; Figure S3, density of states (DOS) of the QD-**1** and QD-**2** complexes, along with the projection (PDOS) on the QD core and the ligand shell; Figure S4, bonding/antibonding character of the band edge molecular orbitals of the QD-**1** and QD-**2** complexes; Figure S5, density of states (DOS) of the QD-**1** and QD-**2** complexes, along with the projection on the Cd/Se atoms and on the anchoring/appending moieties of the surface ligands; Figure S6, Gaussian fit of the first excitonic feature of the QD-**1** and QD-**2** complexes; Figures S7 and S8, partition of the optical spectra of the QD-**1** and QD-**2** complexes (PDF)

■ AUTHOR INFORMATION

Corresponding Authors

*E-mail: jmkimteo@gmail.com (J.M.A.).
*E-mail: filippo@thch.unipg.it (F.D.A.).

Notes

The authors declare no competing financial interest.

■ ACKNOWLEDGMENTS

J.M.A. would like to thank Eusko Jaurlaritza (Basque Government) for funding through a postdoc fellowship.

■ REFERENCES

(1) Murphy, C. J.; Coffer, J. L. Quantum Dots: A Primer. *Appl. Spectrosc.* **2002**, *56*, 16−27.
(2) Alivisatos, A. P. Semiconductor Clusters, Nanocrystals, and Quantum Dots. *Science* **1996**, *271*, 933−937.
(3) Alivisatos, A. P. Perspectives on the Physical Chemistry of Semiconductor Nanocrystals. *J. Phys. Chem.* **1996**, *100*, 13226−13239.
(4) Voznyy, O.; Zhitomirsky, D.; Stadler, P.; Ning, Z.; Hoogland, S.; Sargent, E. H. A Charge-Orbital Balance Picture of Doping in Colloidal Quantum Dot. *ACS Nano* **2012**, *6*, 8448−8455.
(5) Voznyy, O.; Thon, S. M.; Ip, A. H.; Sargent, E. H. Dynamic Trap Formation and Elimination in Colloidal Quantum Dots. *J. Phys. Chem. Lett.* **2013**, *4*, 987−992.
(6) Voznyy, O.; Sargent, E. H. Atomistic Model of Fluorescence Intermittency of Colloidal Quantum Dots. *Phys. Rev. Lett.* **2014**, *112*, 157401.
(7) Thon, S. M.; Ip, A. H.; Voznyy, O.; Levina, L.; Kemp, K. W.; Carey, G. H.; Masala, S.; Sargent, E. H. Role of Bond Adaptability in the Passivation of Colloidal Quantum Dot Solids. *ACS Nano* **2013**, *7*, 7680−7688.
(8) Hines, D. A.; Kamat, P. V. Recent Advances in Quantum Dot Surface Chemistry. *ACS Appl. Mater. Interfaces* **2014**, *6*, 3041−3057.
(9) Prezhdo, O. V. Photoinduced Dynamics in Semiconductor Quantum Dots: Insights from Time-Domain Ab Initio Studies. *Acc. Chem. Res.* **2009**, *42*, 2005−2016.
(10) Jasieniak, J.; Califano, M.; Watkins, S. E. Size-Dependent Valence and Conduction Band-Edge Energies of Semiconductor Nanocrystals. *ACS Nano* **2011**, *5*, 5888−5902.
(11) Azpiroz, J. M.; Mosconi, E.; Ugalde, J. M.; De Angelis, F. Effect of Structural Dynamics on the Opto-Electronic Properties of Bare and Hydrated ZnS QDs. *J. Phys. Chem. C* **2014**, *118*, 3274−3284.
(12) Kalyuzhny, G.; Murray, R. W. Ligand Effects on Optical Properties of CdSe Nanocrystals. *J. Phys. Chem. B* **2005**, *109*, 7012−7021.
(13) Kilina, S.; Ivanov, S.; Tretiak, S. Effect of Surface Ligands on Optical and Electronic Spectra of Semiconductor Nanoclusters. *J. Am. Chem. Soc.* **2009**, *131*, 7717−7726.
(14) Munro, A. M.; Jen-LaPlante, I.; Ng, M. S.; Ginger, D. S. Quantitative Study of the Effects of Surface Ligand Concentration on CdSe Nanocrystal Photoluminescence. *J. Phys. Chem. C* **2007**, *111*, 6220−6227.
(15) Wei, H. H.-Y.; Evans, C. M.; Swartz, B. D.; Neukirch, A. J.; Young, J.; Prezhdo, O. V.; Krauss, T. D. Colloidal Semiconductor Quantum Dots with Tunable Surface Composition. *Nano Lett.* **2012**, *12*, 4465−4471.
(16) Harris, C.; Kamat, P. V. Photocatalysis with CdSe Nanoparticles in Confined Media: Mapping Charge Transfer Events in the Subpicosecond to Second Timescales. *ACS Nano* **2009**, *3*, 682−690.
(17) Harris, C.; Kamat, P. V. Photocatalytic Events of CdSe Quantum Dots in Confined Media. Electrodic Behavior of Coupled Platinum Nanoparticles. *ACS Nano* **2010**, *4*, 7321−7330.

DOI: 10.1021/acsami.5b05418
ACS Appl. Mater. Interfaces 2015, 7, 19736−19745

(18) Tseng, H.-W.; Wilker, M. B.; Damrauer, N. H.; Dukovic, G. Charge Transfer Dynamics between Photoexcited CdS Nanorods and Mononuclear Ru Water-Oxidation Catalysts. *J. Am. Chem. Soc.* **2013**, *135*, 3383−3386.
(19) Ruberu, T. P. A.; Nelson, N. C.; Slowing, I. I.; Vela, J. Selective Alcohol Dehydrogenation and Hydrogenolysis with Semiconductor-Metal Photocatalysts: Toward Solar-to-Chemical Energy Conversion of Biomass-Relevant Substrates. *J. Phys. Chem. Lett.* **2012**, *3*, 2798−2802.
(20) Wang, C.; Thompson, R. L.; Baltrus, J.; Matranga, C. Visible Light Photoreduction of CO2 Using CdSe/Pt/TiO2 Heterostructured Catalysts. *J. Phys. Chem. Lett.* **2010**, *1*, 48−53.
(21) Kamat, P. V. Quantum Dot Solar Cells. Semiconductor Nanocrystals as Light Harvesters. *J. Phys. Chem. C* **2008**, *112*, 18737−18753.
(22) Jun, H. K.; Careem, M. A.; Arof, A. K. Quantum Dot-Sensitized Solar Cells-Perspective and Recent Developments: A Review of Cd Chalcogenide Quantum Dots as Sensitizers. *Renewable Sustainable Energy Rev.* **2013**, *22*, 148−167.
(23) Hines, D. A.; Becker, M. A.; Kamat, P. V. Photoinduced Surface Oxidation and Its Effect on the Exciton Dynamics of CdSe Quantum Dots. *J. Phys. Chem. C* **2012**, *116*, 13452−13457.
(24) Hines, D. A.; Kamat, P. V. Quantum Dot Surface Chemistry: Ligand Effects and Electron Transfer Reactions. *J. Phys. Chem. C* **2013**, *117*, 14418−14426.
(25) Dibbell, R. S.; Youker, D. G.; Watson, D. F. Excited-State Electron Transfer from CdS Quantum Dots to TiO2 Nanoparticles via Molecular Linkers with Phenylene Bridges. *J. Phys. Chem. C* **2009**, *113*, 18643−18651.
(26) Querner, C.; Reiss, P.; Bleuse, J.; Pron, A. Chelating Ligands for Nanocrystals' Surface Functionalization. *J. Am. Chem. Soc.* **2004**, *126*, 11574−11582.
(27) Zotti, G.; Vercelli, B.; Berlin, A.; Virgili, T. Multilayers of CdSe Nanocrystals and Bis(dithiocarbamate) Linkers Displaying Record Photoconduction. *J. Phys. Chem. C* **2012**, *116*, 25689−25693.
(28) Frederick, M. T.; Amin, V. A.; Cass, L. C.; Weiss, E. A. A Molecule to Detect and Perturb the Confinement of Charge Carriers in Quantum Dots. *Nano Lett.* **2011**, *11*, 5455−60.
(29) Frederick, M. T.; Amin, V. A.; Swenson, N. K.; Ho, A. Y.; Weiss, E. A. Control of Exciton Confinement in Quantum Dot-Organic Complexes through Energetic Alignment of Interfacial Orbitals. *Nano Lett.* **2013**, *13*, 287−92.
(30) Frederick, M. T.; Weiss, E. A. Relaxation of Exciton Confinement in CdSe Quantum Dots by Modification with a Conjugated Dithiocarbamate Ligand. *ACS Nano* **2010**, *4*, 3195−200.
(31) Teunis, M. B.; Dolai, S.; Sardar, R. Effects of Surface-Passivating Ligands and Ultrasmall CdSe Nanocrystal Size on the Delocalization of Exciton Confinement. *Langmuir* **2014**, *30*, 7851−7858.
(32) Tan, Y.; Jin, S.; Hamers, R. J. Photostability of CdSe Quantum Dots Functionalized with Aromatic Dithiocarbamate Ligands. *ACS Appl. Mater. Interfaces* **2013**, *5*, 12975−12983.
(33) Jin, S.; Harris, R. D.; Lau, B.; Aruda, K. O.; Amin, V. a.; Weiss, E. a. Enhanced Rate of Radiative Decay in CdSe Quantum Dots upon Adsorption of an Exciton-Delocalizing Ligand. *Nano Lett.* **2014**, *14*, 5323−5328.
(34) Fritzinger, B.; Capek, R. K.; Lambert, K.; Martins, C.; Hens, Z. Utilizing Self-Exchange To Address the Binding of Carboxylic Acid Ligands to CdSe Quantum Dots. *J. Am. Chem. Soc.* **2010**, *132*, 10195−10201.
(35) Car, R.; Parrinello, M. Unified Approach for Molecular Dynamics and Density-Functional Theory. *Phys. Rev. Lett.* **1985**, *55*, 2471−2474.
(36) Perdew, J. P.; Burke, K.; Ernzerhof, M. Generalized Gradient Approximation Made Simple. *Phys. Rev. Lett.* **1996**, *77*, 3865−3868.
(37) Giannozzi, P.; De Angelis, F.; Car, R. First-Principle Molecular Dynamics with Ultrasoft Pseudopotentials: Parallel Implementation and Application to Extended Bioinorganic Systems. *J. Chem. Phys.* **2004**, *120*, 5903−5915.
(38) Pasquarello, A.; Laasonen, K.; Car, R.; Lee, C.; Vanderbilt, D. Ab Initio Molecular Dynamics for d-Electron Systems: Liquid Copper at 1500 K. *Phys. Rev. Lett.* **1992**, *69*, 1982−1985.
(39) Giannozzi, P.; Baroni, S.; Bonini, N.; Calandra, M.; Car, R.; Cavazzoni, C.; Ceresoli, D.; Chiarotti, G. L.; Cococcioni, M.; Dabo, I.; Dal Corso, A.; de Gironcoli, S.; Fabris, S.; Fratesi, G.; Gebauer, R.; Gerstmann, U.; Gougoussis, C.; Kokalj, A.; Lazzeri, M.; Martin-Samos, L.; Marzari, N.; Mauri, F.; Mazzarello, R.; Paolini, S.; Pasquarello, A.; Paulatto, L.; Sbraccia, C.; Scandolo, S.; Sclauzero, G.; Seitsonen, A. P.; Smogunov, A.; Umari, P.; Wentzcovitch, R. M. QUANTUM ESPRESSO: a Modular and Open-Source Software Project for Quantum Simulations of Materials. *J. Phys.: Condens. Matter* **2009**, *21*, 395502.
(40) Stevens, W. J.; Krauss, M.; Basch, H.; Jasien, P. G. Relativistic Compact Effective Potentials and Efficient, Shared-Exponent BasisSets for the 3rd-Row, 4th-Row, and 5th-Row Atoms. *Can. J. Chem.* **1992**, *70*, 612−630.
(41) Ahlrichs, R.; Bar, M.; Haser, M.; Horn, H.; Kolmel, C. Electronic-Structure Calculations on Workstation Computers - The Program System Turbomole. *Chem. Phys. Lett.* **1989**, *162*, 165−169.
(42) Azpiroz, J. M.; Ugalde, J. M.; Infante, I. Benchmark Assessment of Density Functional Methods on Group II-VI MX (M = Zn, Cd; X = S, Se, Te) Quantum Dots. *J. Chem. Theory Comput.* **2014**, *10*, 76−89.
(43) Adamo, C.; Barone, V. Toward Reliable Density Functional Methods without Adjustable Parameters: The PBE0Model. *J. Chem. Phys.* **1999**, *110*, 6158−6170.
(44) Klamt, A. Conductor-Like Screening Model for Real Solvents: A New Approach to the Quantitative-Calculation of Solvation Phenomena. *J. Phys. Chem.* **1995**, *99*, 2224−2235.
(45) Grimme, S. A Simplified Tamm-Dancoff Density Functional Approach for the Electronic Excitation Spectra of Very Large Molecules. *J. Chem. Phys.* **2013**, *138*, 244104.
(46) Voznyy, O. Mobile Surface Traps in CdSe Nanocrystals with Carboxylic Acid Ligands. *J. Phys. Chem. C* **2011**, *115*, 15927−15932.
(47) Koposov, A. Y.; Cardolaccia, T.; Albert, V.; Badaeva, E.; Kilina, S.; Meyer, T. J.; Tretiak, S.; Sykora, M. Formation of Assemblies Comprising Ru-Polypyridine Complexes and CdSe Nanocrystals Studied by ATR-FTIR Spectroscopy and DFT Modeling. *Langmuir* **2011**, *27*, 8377−8383.
(48) Schapotschnikow, P.; Hommersom, B.; Vlugt, T. J. H. Adsorption and Binding of Ligands to CdSe Nanocrystals. *J. Phys. Chem. C* **2009**, *113*, 12690−12698.
(49) Puzder, A.; Williamson, A. J.; Gygi, F.; Galli, G. Self-Healing of CdSe Nanocrystals: First-Principles Calculations. *Phys. Rev. Lett.* **2004**, *92*, 217401.
(50) Azpiroz, J. M.; Mosconi, E.; Angelis, F. D. Modeling ZnS and ZnO Nanostructures: Structural, Electronic, and Optical Properties. *J. Phys. Chem. C* **2011**, *115*, 25219−25226.
(51) Ronca, E.; Pastore, M.; Belpassi, L.; Tarantelli, F.; De Angelis, F. Influence of the Dye Molecular Structure on the TiO2 Conduction Band in Dye-Sensitized Solar Cells: Disentangling Charge Transfer and Electrostatic Effects. *Energy Environ. Sci.* **2013**, *6*, 183−193.
(52) Lee, J. R. I.; Whitley, H. D.; Meulenberg, R. W.; Wolcott, A.; Zhang, J. Z.; Prendergast, D.; Lovingood, D. D.; Strouse, G. F.; Ogitsu, T.; Schwegler, E.; Terminello, L. J.; van Buuren, T. Ligand-Mediated Modification of the Electronic Structure of CdSe Quantum Dots. *Nano Lett.* **2012**, *12*, 2763−2767.
(53) Azpiroz, J. M.; Matxain, J. M.; Infante, I.; Lopez, X.; Ugalde, J. M. A DFT/TDDFT Study on the Optoelectronic Properties of the Amine-Capped Magic (CdSe)13 Nanocluster. *Phys. Chem. Chem. Phys.* **2013**, *15*, 10996−11005.
(54) Giansante, C.; Infante, I.; Fabiano, E.; Grisorio, R.; Suranna, G. P.; Gigli, G. 'Darker-than-Black' PbS Quantum Dots: Enhancing Optical Absorption of Colloidal Semiconductor Nanocrystals via Short Conjugated Ligands. *J. Am. Chem. Soc.* **2015**, *137*, 1875−1886.
(55) Efros, A. L.; Rosen, M. The Electronic Structure of Semiconductor Nanocrystals. *Annu. Rev. Mater. Sci.* **2000**, *30*, 475−521.

DOI: 10.1021/acsami.5b05418
ACS Appl. Mater. Interfaces 2015, 7, 19736−19745

(56) Boehme, S. C.; Azpiroz, J. M.; Aulin, Y. V.; Grozema, F. C.; Vanmaekelbergh, D.; Siebbeles, L. D. a.; Infante, I.; Houtepen, A. J. Density of Trap States and Auger-mediated Electron Trapping in CdTe Quantum-Dot Solids. *Nano Lett.* **2015**, *15*, 3056−3066.
(57) Sandeep, C. S. S.; Azpiroz, J. M.; Evers, W. H.; Boehme, S. C.; Moreels, I.; Kinge, S.; Siebbeles, L. D. A.; Infante, I.; Houtepen, A. J. Epitaxially Connected PbSe Quantum-Dot Films: Controlled Neck Formation and Optoelectronic Properties. *ACS Nano* **2014**, *8*, 11499−11511.

DOI: 10.1021/acsami.5b05418
ACS Appl. Mater. Interfaces 2015, 7, 19736−19745